# Tunneling Induced by Longitudinal Microwave Phonons in Al-Pb, Al-Sn, and Pb-Pb Superconducting Diodes

Y. GOLDSTEIN,* B. ABELES, AND ROGER W. COHEN
*RCA Laboratories, Princeton, New Jersey*
(Received 9 June 1966)

Measurements are presented of the change $\Delta I_s(V)$ in the tunneling current $I(V)$ in superconducting diodes due to longitudinal microwave phonons as a function of voltage bias $V$, acoustic power, and temperature. The measurements were performed on Al-Pb, Al-Sn, and Pb-Pb diodes in the temperature range 1.3–2.1°K. The voltage dependence, which was heretofore thought to be described by $\Delta I_s(V) \propto d^2I/dV^2$, was found to exhibit departures from this law. This effect is most striking in Pb-Pb diodes and somewhat less apparent when one of the superconductors making up the diode is aluminum. Furthermore, the magnitude of the measured $\Delta I_s$ is much larger than one would predict from present theory. The tunnel-diode current-pulse echoes exhibit a nonexponential decay which is strongly temperature-dependent. None of this behavior is predicted by the theory.

## I. INTRODUCTION

IT was found recently that coherent microwave phonons appreciably affect the current-voltage characteristics of superconducting tunnel diodes.[1–4] The extra current $\Delta I_s(V)$ in superconducting Al-Pb diodes due to longitudinal phonons resembled closely the second derivative of the $I$-$V$ characteristic in the absence of sound.[1–4] On the other hand, for transverse phonons, it was shown that $\Delta I_s$ had a bias dependence which suggested heating of the tunnel diode by absorption of transverse microwave phonons.[5]

In this paper we report further work on the effect of *longitudinal* microwave phonons on superconducting Al-Pb diodes as well as on Al-Sn and Pb-Pb diodes. A detailed description of the experimental techniques is given. The experimental results are compared with theoretical predictions.

## II. EXPERIMENTAL TECHNIQUES

The tunnel diodes were prepared by vapor deposition of Al, Pb, or Sn in the form of cross-strips on a $\frac{5}{16}$-in.-diam end face of an $X$-cut quartz rod. The quartz rods were 1-in. long, step ground with a $\frac{5}{16}$-in. diam for $\frac{11}{16}$ in. of its length and the remaining $\frac{5}{16}$ in. of its length ground down to a diameter of $\frac{1}{8}$ of an inch. The end faces were polished flat and parallel to within optical tolerances.

The Al-Pb and Al-Sn diodes were made as follows: A strip of aluminum, 0.15 cm wide and 500 Å thick was deposited at the rate of 20 Å/sec. Next, the aluminum was oxidized for 30 sec in a dry oxygen atmosphere and a 0.1-cm-wide lead or tin strip was deposited on top of the aluminum oxide at a deposition rate of 50 Å/sec. The tin films were 3000-Å thick. The lead strips were made in two different thicknesses: 1500 Å or 7000 Å. In the Pb-Pb diodes, both strips were 1500 Å thick and 0.025 cm wide. The lead film, deposited first, was oxidized in a dry oxygen atmosphere for 16 h at a temperature of 46°C.

The $\frac{1}{8}$-in. diam of the rod was inserted into a reentrant microwave cavity. Sound waves were excited in the rod using standard pulse-echo techniques. A schematic diagram of the experimental setup is shown in Fig. 1. Most of the measurements were made at $X$-band frequencies, with the resonant frequency of the cavity near 9 GHz. The microwave transmitter used was a QK790 magnetron with 1-kW peak power. The microwave power was fed into the cavity in pulses of 1 $\mu$sec duration at a repetition rate of 500 pulses/sec. The cavity gap (0.090 in.) and the center-post diameter (0.16 in.) were large to ensure that the electric field distribution across the face of the quartz rod was as uniform as possible. The electric field at the surface of the quartz rod launched a pulse of longitudinal phonons which was reflected back and forth by the end faces. The sound echoes gave rise to microwave pulses in the cavity, which were detected by a superheterodyne receiver and displayed on a dual trace scope. The

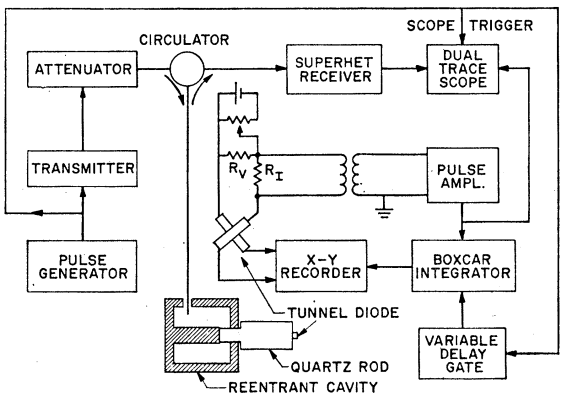


FIG. 1. Block diagram of experimental setup.

* Present address: The Hebrew University, Jerusalem, Israel.

[1] B. Abeles and Y. Goldstein, postdeadline paper presented at the meeting of the American Physical Society, Berkeley, California, 1964 (unpublished); Y. Goldstein and B. Abeles, Phys. Letters 14, 78 (1965).

[2] E. Lax and F. L. Vernon, Jr., Bull. Am. Phys. Soc. 9, 713 (1964).

[3] E. Lax and F. L. Vernon, Jr., Phys. Rev. Letters 14, 256 (1965).

[4] B. Abeles and Y. Goldstein, Phys. Rev. Letters 14, 595 (1965).

[5] B. Abeles and Y. Goldstein, Phys. Letters 18, 11 (1965).

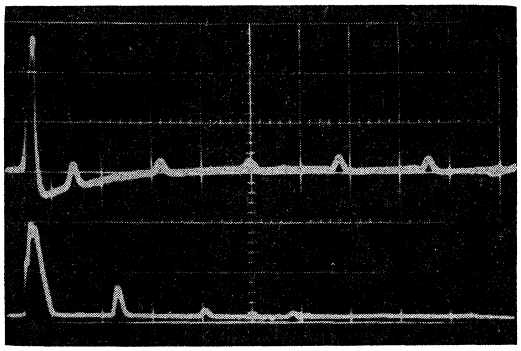

FIG. 2. Typical oscillogram of tunnel-diode current pulses $\Delta I_s^*$ at output of pulse amplifier (upper trace) and of sound echoes detected by microwave receiver (lower trace). Horizontal scale 5 $\mu$sec/division, diode Al-Pb, thickness of Pb strip 7000 Å, $T=1.3$°K.

conversion efficiency of microwave power to sound power was about $10^{-4}$.

A variable dc voltage bias source was provided for the tunnel diode by passing a current through a small resistor ($R_V\sim 0.3\ \Omega$) in parallel with the diode. The tunneling current was measured as voltages across a series resistance $R_I\sim 5\ \Omega$. In order to minimize electrical pick up as well as to enable the tracing out of the diode characteristics in the negative resistance region, both $R_I$ and $R_V$ were placed in the cryostat close to the diode.

The microwave pulses gave rise to current pulses in the tunnel diode, which were fed through a pulse transformer to a pulse amplifier. The transformer, connected across $R_I$ outside the cryostat, served two purposes. Its 1:30 primary to secondary winding ratio provided an impedance match between the low output impedance of the tunnel diode and the high amplifier input impedance. It also isolated the diode circuit from electrical ground; this helped to reduce the electrical pickup originating from the transmitter power supply.

An oscillogram of pulse trains due to a single microwave excitation pulse is shown in Fig. 2. The lower trace is a succession of sound echoes detected by the microwave receiver. The first pulse on this trace arises from microwave radiation picked up by the receiver. The spacing of the succeeding echoes corresponds to twice the time of flight of a sound wave through the rod. The upper trace is the output of the current-pulse amplifier. The first current pulse is coincident with the microwave transmitter pulse and is due to the microwave radiation leaking out of the cavity and interacting directly with the tunnel diode. The subsequent current pulses are coincident with the arrival of the sound pulses at the tunnel diode and are due to an interaction of sound waves with the diode. The undershoot of the trace is due to the low-frequency cutoff of the pulse amplifier. To plot the voltage-bias dependence of a current pulse due to a particular sound echo, the output of the pulse amplifier was fed into a boxcar integrator, which was gated by a 0.6-$\mu$sec wide gate synchronous with the arrival of the sound echo at the tunnel diode. The output of the boxcar integrator, which was proportional to the amplitude of the current pulse, was plotted on an $X$-$Y$ recorder as a function of the bias voltage on the diode.

$I$-$V$ characteristics were measured by connecting the $X$-$Y$ recorder directly across $R_I$. To determine the dynamic conductance $\sigma=dI/dV$, a voltage of 10-$\mu$V amplitude at 1 kHz was applied across $R_V$, and $R_I$ was shunted by a sufficiently small resistance $r$ so that $\sigma\{R_V+[rR_I/(R_I+r)]\}\ll 1$. Under these conditions, the amplitude of the ac voltage detected across $R_I$ was proportional to $\sigma$.

The information to be extracted from the measurements is the tunneling current in the presence of microwave phonons $I_s(V)$ or the extra current $\Delta I_s(V)$:

$$\Delta I_s(V)=I_s(V)-I(V), \tag{1}$$

where $I(V)$ is the tunneling current in the absence of microwave phonons and $V$ is the dc bias voltage. Since the tunnel diode is terminated by a load resistance, the actual measured extra current $\Delta I_s^*$ is given by

$$\Delta I_s^*=I_s(V-R_L\Delta I_s^*)-I(V), \tag{2}$$

where $(-R_L\Delta I_s^*)$ is the voltage drop on the load resistance:

$$R_L=R_V+R_PR_I/(R_P+R_I). \tag{3}$$

The resistors $R_I$ and $R_V$ are defined in Fig. 1, and $R_P$ is the pulse impedance of the transformer in Fig. 1 ($R_P=3.6\ \Omega$).

To determine $\Delta I_s(V)$ we expand the right-hand side of Eq. (2) in a power series in $R_L\Delta I_s^*$, neglect all but the linear term in $R_L\Delta I_s^*$ and obtain the differential equation

$$\Delta I_s=[1+R_L\sigma+R_Ld(\Delta I_s)/dV]\Delta I_s^*. \tag{4}$$

The condition for neglecting the second-order term is

$$\Delta I_s^*\ll(2/R_L)(dI_s/dV)/(d^2I/dV^2). \tag{5}$$

This condition was satisfied for all the measurements reported in this paper.

For low microwave powers, the third term on the right side of Eq. (4) can be neglected and, therefore,

$$\Delta I_s=(1+R_L\sigma)\Delta I_s^*. \tag{6}$$

Furthermore, it should be noted that when $\Delta I_s$ has an extremum, Eq. (4) reduces exactly to Eq. (6). In general, however, Eq. (4) must be integrated numerically using the measured values of $\Delta I_s^*$, $\sigma$, and $R_L$.

## III. THEORY

The interaction of electromagnetic radiation of angular frequency $\omega$ with a superconducting tunnel diode has been treated on the basis of three different

models. Cohen, Falicov, and Phillips[6] assumed that the effect of the radiation is to modulate the energy gap of the superconductors. Tien and Gordon[7] used the Schrödinger equation to calculate the modulation of the single-particle wave functions obtained by adding a term

$$H'=v\cos\omega t \tag{7}$$

to the Hamiltonian of one metal. Riedel[8] considered the effect of a perturbation of the form (7) on a BCS superconductor. The three approaches yield similar expressions for the current $I_R$ in the presence of radiation. In the limit of long wavelengths, so that spatial variation of the parameter $v$ may be ignored, $I_R$ is given by

$$I_R(V)=\sum_{n=-\infty}^{\infty} J_n^2(\alpha_R)I(V+n\hbar\omega), \tag{8}$$

where

$$\alpha_R=v/\hbar\omega \tag{9}$$

and $I$ is the current in the absence of radiation.

A heuristic extension of Eq. (8) to the case of coherent acoustic waves was made by Lax and Vernon.[3] They replaced the parameter $v$ in Eq. (9) by $(c_1s_1-c_2s_2)$, where $c_i$ and $s_i$ are, respectively, the deformation potentials and strains in the two metals. In the following we will discuss the conditions under which this extension is valid.

The effect of coherent acoustic waves on a superconducting tunnel diode can be treated in a similar manner as Riedel's treatment of the photon case. The BCS Hamiltonian for one superconductor is

$$H_{\mathrm{BCS}}=\sum_{k\sigma}\epsilon_k a_{k\sigma}^{\dagger}a_{k\sigma}-U\sum_{kk'}b_{k'}^{\dagger}b_k\eta(\epsilon_k)\eta(\epsilon_{k'}) \tag{10}$$

$$b_k=a_{k\uparrow}a_{-k\downarrow} \tag{10a}$$

$$\eta(\epsilon_k)=+1 \quad \text{for} \quad |\epsilon_k|\leq\hbar\Theta$$
$$=0 \quad \text{otherwise}. \tag{10b}$$

Here $a_{k\sigma}$ and $a_{k\sigma}^{\dagger}$ are, respectively, destruction and creation operators for electrons of momentum $\mathbf{k}$ and spin $\sigma$, $\epsilon_k$ is the single-particle energy measured from the Fermi surface, and $U$ is the strength of the electron-phonon interaction. The functions $\eta$ fix the position of the electron-phonon interaction in $k$ space to within a spherical shell of thickness (in energy) $2\Theta$, where $\Theta$ is an average phonon frequency of the order of the Debye frequency. We wish to treat the effect of longitudinal acoustic waves of wave vector $\mathbf{q}$ perpendicular to the plane of the diode and frequency $\omega=v_sq$ ($v_s$ being the sound velocity) on a system of electrons which is described by the Hamiltonian (10). In the case where the wavelength of the impressed phonons is much smaller than the electronic mean free path $l$ ($ql\gg1$), only those electrons whose $\mathbf{k}\perp\mathbf{q}$ interact with the phonons because of the requirements of conservation of energy and momentum. However, the electrons which participate in tunneling are confined to a relatively narrow cone about the normal to the junction surface. Therefore, for these electrons, the interactions with the phonons is very small, and no detectable change in the tunneling current is expected. Hence, only the situation $ql\ll1$ need be considered. In this case the compressional wave produces a modulation of the electron density and a corresponding modulation of the electronic energies of the form

$$\epsilon_k\longrightarrow\epsilon_k+cs\cos\omega t, \tag{11}$$

where $c=\frac{2}{3}\epsilon_F$ and $\epsilon_F$ is the Fermi energy. Thus, one can replace the single-particle energies $\epsilon_k$ in the first term on the right side of Eq. (10) by the modified spectrum (11). Furthermore, if the electron-phonon interaction is able to follow the acoustic wave instantaneously, one can also replace the argument of the $\eta$ functions by the spectrum (11). Since the electron-phonon interaction is retarded over times of the order of the inverse of the Debye frequency, one expects this latter modification to be valid if

$$\omega\ll\Theta. \tag{12}$$

In the experiments described in this paper, $\omega/\Theta\sim10^{-3}$, so that condition (12) is very well satisfied. Hence, provided the magnitude of $U$ does not change, the Hamiltonian in the presence of long-wavelength longitudinal acoustic phonons can be written in the form

$$H=H_{\mathrm{BCS}}\big|_{\epsilon_k\to\epsilon_k+cs\cos\omega t}. \tag{13}$$

The Hamiltonian (13) is of the form considered by Riedel with the parameter $v$ replaced by $cs$. The calculation of the current $I_s$ in the presence of acoustic excitation proceeds exactly as in the case of electromagnetic radiation with the result

$$I_s(V)=\sum_{n=-\infty}^{+\infty} J_n^2(\alpha_s)I(V+n\hbar\omega), \tag{14}$$

where

$$\alpha_s=\frac{\delta(cs)}{\hbar\omega}=\frac{c_1s_1-c_2s_2}{\hbar\omega}. \tag{15}$$

Here the subscripts 1 and 2 refer to metal 1 and metal 2, respectively.

It should be pointed out that Eq. (14) is only valid if the energy-gap parameters $\Delta_i$ of the two superconductors are unchanged by the acoustic waves. This assumption is expected to be valid if

$$cs\ll\Delta, \tag{16a}$$

$$\hbar\omega\ll\Delta. \tag{16b}$$

[6] M. H. Cohen, L. M. Falicov, and J. C. Phillips, in *Proceedings of the Eighth International Conference on Low-Temperature Physics, London, 1962*, edited by R. O. Davies (Butterworths Scientific Publications Ltd., London, 1963), p. 163.

[7] P. K. Tien and J. P. Gordon, Phys. Rev. **129**, 647 (1963).

[8] Von Eberhard Riedel, Z. Naturforsch. **19a**, 1634 (1964).

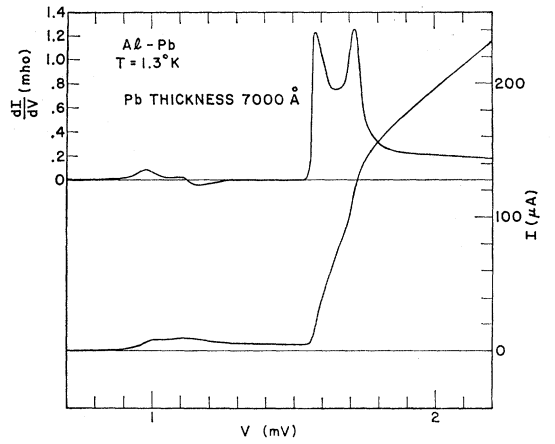


FIG. 3. $I$-$V$ and $dI/dV$ characteristics of Al-Pb diode measured at 1.3°K. The thickness of the Pb strip is 7000 Å.

The conditions (16) imply that the sound wave does not alter the number of excited quasiparticles in an isolated superconductor; that is, none of the Cooper pairs are broken up to form quasiparticles.

It is of interest to consider the form of Eq. (14) in the limits of: (a) low acoustic power ($\alpha_s \ll 1$) and (b) low applied frequency ($\omega \to 0$). In case (a) it is necessary to retain only the term $n=\pm 1, 0$ in the summation. Using the small argument expansion of the Bessel functions, one readily obtains the following result for the change in current due to acoustic excitation $\Delta I_s = I_s - I$:

$$\Delta I_s(V) = (\alpha_s^2/4)[I(V+\hbar\omega)+I(V-\hbar\omega)-2I(V)], \quad \alpha_s \ll 1. \quad (17)$$

If one expands the right side of Eq. (17) in a power series in $\hbar\omega$, the first two nonvanishing terms yield

$$\Delta I_s(V) \approx \frac{[\delta(cs)]^2}{4}\left\{\frac{d^2I(V)}{dV^2}+\frac{(\hbar\omega)^2}{12}\frac{d^4I(V)}{dV^4}\right\}, \quad \alpha_s \approx 1. \quad (18)$$

From Eq. (18) one sees that the leading term is independent of frequency and proportional to the second derivative[9] of the unperturbed diode current. The frequency enters only in terms involving fourth and higher derivatives of $I(V)$.

To evaluate the limit $\omega \to 0$ [case (b)], one must sum over all values of $n$ since $\alpha_s \to \infty$. The summation is performed in the Appendix and the result is

$$I_s(V) = I_0(\delta[cs]d/dV)I(V), \quad \omega \to 0, \quad (19)$$

where $I_0$ is the modified Bessel function of order zero. The Bessel function is understood to be a power-series operator which operates on the function $I(V)$. The first few terms in the power-series expansion yield

$$\Delta I_s(V) \approx \frac{[\delta(cs)]^2}{4}\frac{d^2I(V)}{dV^2}+\frac{[\delta(cs)]^4}{64}\frac{d^4I(V)}{dV^4}+\frac{[\delta(cs)]^6}{2304}\frac{d^6I(V)}{dV^6}. \quad (20)$$

In the next section, we shall present experimental results and compare them with the predictions of the above theory. For this purpose, $\Delta I_{s,r}$ was computed from Eqs. (8), (9), (14), and (15) as a function of $\alpha_{s,r}$ and $V$ using the actual diode $I$-$V$ curves as input data. It should be mentioned that in the case of identical metals, $\delta(cs)=0$ and therefore $\Delta I_s=0$. In order to obtain a nonvanishing result, one must assume $\delta(cs)\neq 0$. This may arise, for example, from a phase difference between the strains in the two metals. Since, for some of the diodes to be described in the next section, the phonon wavelength was of the order of the film thickness, such phase shifts are present.

## IV. DISCUSSION OF EXPERIMENTAL RESULTS

### A. Diode Characteristics

Results are presented of measurements on four Al-Pb diodes, one Al-Sn diode and one Pb-Pb diode. First, we describe some of the characteristic properties of these diodes. The aluminum strips had anomalously

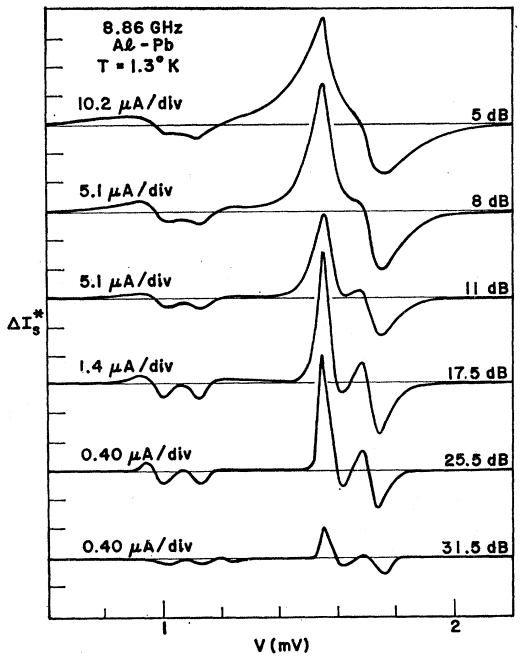


FIG. 4. $X$-$Y$ recorder tracings of the extra current $\Delta I_s^*$ due to 8.86-GHz longitudinal phonons versus bias voltage on a Al-Pb diode at 1.3°K. The relative microwave power levels and the vertical scales are indicated. The $I(V)$ and $dI/dV$ characteristics of this diode are given in Fig. 3.

[9] A similar result was obtained using the simple model in Ref. 4. Comparing Eq. (2) of Ref. 4 with the present Eq. (18) yields for the parameter $\beta$, $\beta = q\delta(cs)/2h\nu$.

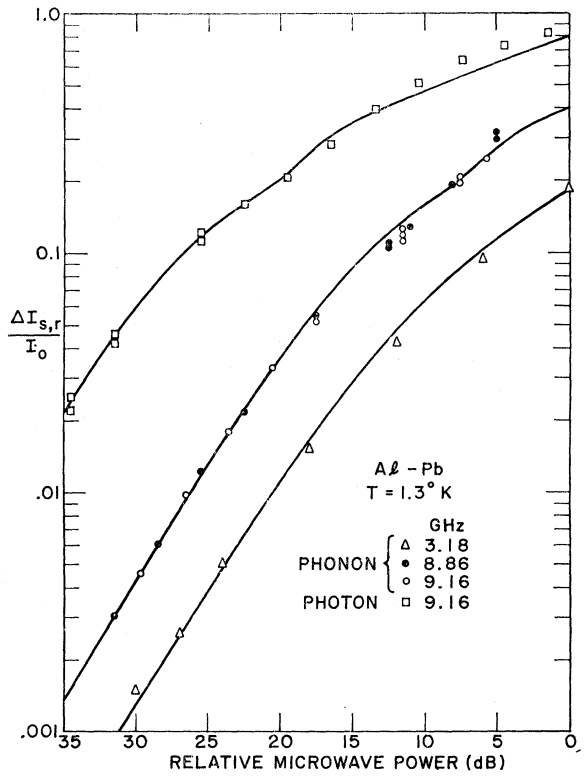


FIG. 5. Normalized, maximum extra current $\Delta I_s/I_0$ due to longitudinal phonons and $\Delta I_r/I_0$ due to photons as a function of relative microwave power at 1.3°K. All the diodes were Al-Pb with 7000-Å-thick lead strips. The bias voltage was kept constant at the value $V_m$ at which $\Delta I_{r,s}$ is maximum. $I_0$ is the current at bias $V_m$, when the diode is normal. The frequencies of the phonons are indicated in the figure.

high transition temperatures of $T_c \approx 2.3$°K. High transition temperatures in thin aluminum films have been previously reported,[1,10,11] but the cause of these high $T_c$'s is not well understood. Using the value of the electronic mean free path $l$ computed from electrical conductivity, it was determined that for all the Al strips $ql \ll 1$, for the 7000-Å-thick Pb strips $ql \gg 1$ and for the 1500-Å-thick Pb strip $ql \approx 1$.

The Al-Pb diodes, in which the lead strips were 7000-Å thick, exhibited double peaks in the conductance curves. In Fig. 3 are shown the $I(V)$ and $dI(V)/dV$ characteristics for an Al-Pb diode in which this effect was most striking. The separation between the peaks is about 130 $\mu$V. Such structure was first observed by Townsend and Sutton[12] and, more recently, by other workers.[4,13] The diodes which had 1500-Å-thick Pb strips (lower part of Fig. 7) did not display this structure. It is thought that this structure may be due to the anisotropy of the Pb energy-gap surface as suggested by Bennett.[14] The results of Bennett's calculations indicate that the two peaks in $dI/dV$ arise from relative maxima of the energy-gap function.

### B. Power Dependence

The bias dependence of the measured extra current $\Delta I_s^*$ for various power levels is shown in Fig. 4. The data was taken at 1.3°K on the Al-Pb diode, whose $I(V)$ and $dI/dV$ characteristics in the absence of sound are shown in Fig. 3. The complex behavior of these curves is associated with the fine structure in the $I$-$V$ curve and is well explained by the theory. At the lowest power levels, Eq. (18) is valid and $\Delta I_s$ behaves essentially as $d^2I/dV^2$. At the highest power levels, Eq. (19) is applicable, so that the higher derivatives of $I$ become important. The effect of these higher derivatives is to produce the observed broadening in the $\Delta I_s^*(V)$ curves.

In Fig. 5 is plotted the normalized extra current $\Delta I_s(V_m)/I_0$ for phonons and $\Delta I_r(V_m)/I_0$ for photons against relative microwave power for three different Al-Pb diodes in which the Pb strip thickness was 7000 Å. The voltage bias was held fixed at the point $V_m$ where the $\Delta I_{s,r}$ had its largest positive value. The quantity $I_0$ is the current at $V_m$ when both metals are in the normal state. The values of $\Delta I_{s,r}$ where obtained from the measured currents $\Delta I_{s,r}^*$ using Eq. (6) to correct for load line effects. The 8.86-GHz and the 9.16-GHz data were obtained on the diodes whose characteristics are given in Fig. 3 and in the upper part of Fig. 7, respectively. The diode on which the 3.8-GHz measurements were made had an $I$-$V$ characteristic very similar to that shown in the upper part of Fig. 7.

The theoretical $\Delta I_{s,r}$, which are denoted by the solid lines, were fitted to the experimental data in the

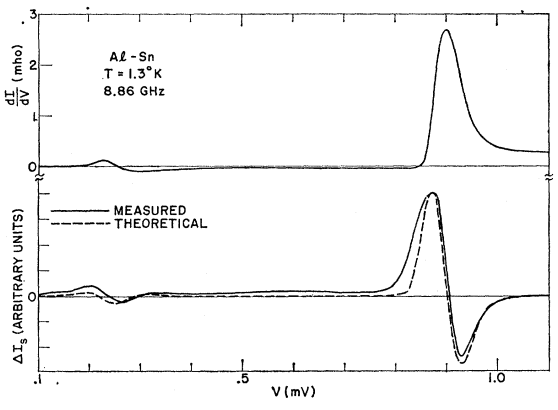


FIG. 6. The extra current $\Delta I_s$ in Al-Sn diode due to 8.86-GHz longitudinal phonons and $dI/dV$ with no phonons as a function of the bias voltage at 1.3°K. The curves are given for the range in which $\Delta I_s$ is linearly proportional to microwave power. The theoretical curve, given by the dashed curve, was computed from Eq. (14) using the measured $I$-$V$ characteristic.

[10] D. H. Douglass, Jr., and R. Meservey, Phys. Rev. 135, A19 (1964).
[11] M. Strongin, O. F. Kammerer, and A. Paskin, Phys. Rev. Letters 14, 949 (1965).
[12] P. Townsend and J. Sutton, Phys. Rev. Letters 11, 154 (1963).
[13] G. I. Rochlin and D. H. Douglass, Jr., Bull. Am. Phys. Soc. 10, 46 (1965); Phys. Rev. Letters 16, 359 (1966).
[14] A. J. Bennet, Phys. Rev. 140, 1902 (1965).

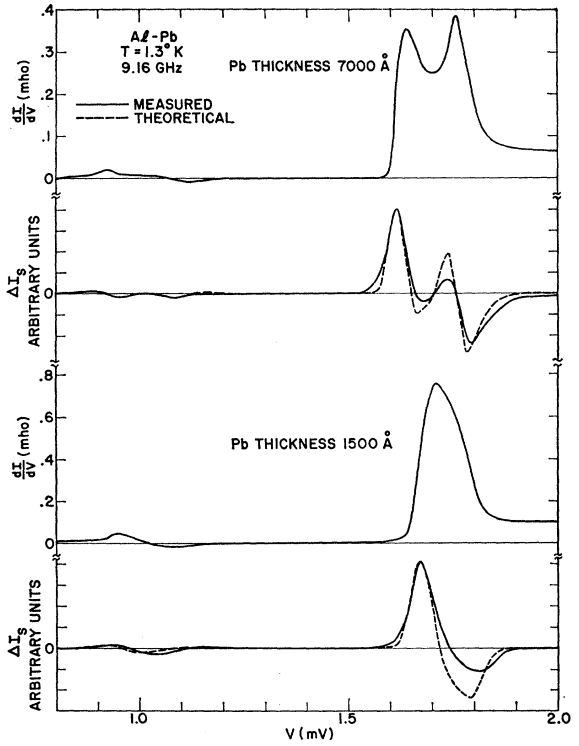


FIG. 7. The extra current $\Delta I_s$ in Al-Pb diodes due to 9.16-GHz longitudinal phonons and $dI/dV$ with no phonons as a function of bias voltage at 1.3°K. The curves are given for the range in which $\Delta I_s$ is linearly proportional to microwave power. The theoretical $\Delta I_s$, given by the dashed curves, was computed from Eq. (14) using the measured $I$-$V$ characteristics. The upper three curves are for a diode with a 7000-Å-thick Pb strip and the lower three curves are for a diode with a 1500-Å-thick Pb strip.

region where both are linear with power. This was accomplished by shifting calculated curves of $\Delta I_{s,r}(\alpha_{s,r}{}^2)$ horizontally until the linear regions coincided with the experimental data. In all cases the agreement between the theory and experiment is remarkably good over the entire range of measurement.

One can obtain an estimate of the magnitude of the strain required to produce the observed $\Delta I_s$. At the highest acoustic power level, the value of $\Delta I_s/I_0$ at 8.86 GHz is approximately 0.3. This corresponds to $\alpha_s \approx 6$. Since $ql \gg 1$ for the Pb film it is assumed that the contribution of the Pb film is negligible (Sec. III). One then obtains from Eq. (15) (with $c_{\mathrm{Al}} = \frac{2}{3}\epsilon_F = 8$ eV) the value $s_{\mathrm{Al}} \approx 3 \times 10^{-5}$. Although the measurements of insertion loss were not very accurate, it appears that the above value of $s_{\mathrm{Al}}$ would require a level of acoustic power more than an order of magnitude larger than was available experimentally.

### C. Dependence on Bias Voltages

In Figs. (6)–(8) are presented the $dI/dV$ curves and the measured and theoretical $\Delta I_s(V)$ characteristics for four diodes in the region where $\Delta I_s$ is linear with power. All the experimental data were corrected for load-line effects using Eq. (6). In all cases, the positive peak values of both the theoretical and measured $\Delta I_s$ occurred at the same bias point. In order to compare the shapes in detail, the curves were scaled so that the values of the $\Delta I_s$ at this point were equal.

There is good agreement with theory for the Al-Pb and the Al-Sn diodes. The agreement is less satisfactory for the Al-Pb diode with the 1500-Å lead strip and the data for the Pb-Pb diode displays a marked departure from the theory. In particular, the ratio of the positive peak to the negative peak is much smaller than that predicted by Eqs. (14) and (15), and the negative peak occurs at a significantly larger bias voltage. Similar effects have been seen in other Pb-Pb diodes on which measurements were made. On the other hand, the bias dependence of the extra current $\Delta I_r$ due to photons agreed well with theory for all the diodes.

### D. Temperature Dependence

The sound echoes produced in the quartz rods used in the present work exhibited a complicated non-exponential decay pattern. This behavior is frequently observed at high acoustic frequencies and may be caused by several different mechanisms.[15] The most

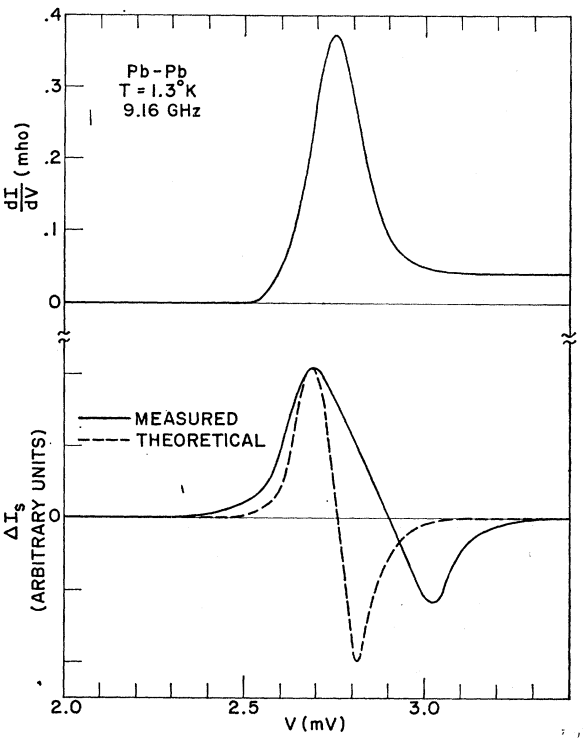


FIG. 8. The extra current $\Delta I_s$ in Pb-Pb diodes due to 9.16-GHz longitudinal phonons and $dI/dV$ with no phonons as a function of bias voltage at 1.3°K. The curves are given for the range in which $\Delta I_s$ is linearly proportional to microwave power. The dashed curve was computed from Eq. (14) using the measured $I$-$V$ characteristic.

[15] E. H. Jacobsen, *Quantum Electronics* (Columbia University Press, New York, 1961), p. 468.

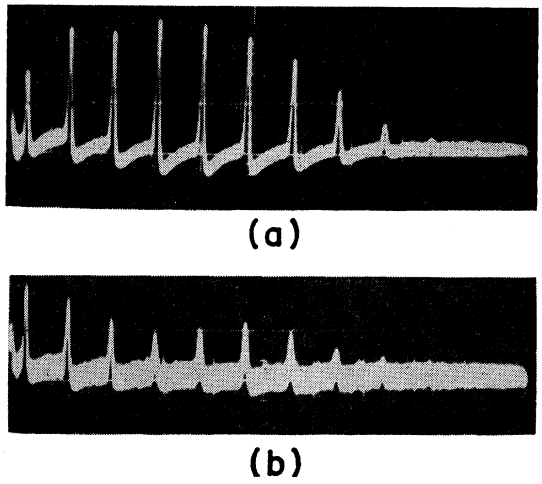


FIG. 9. Oscillograms of current pulses $\Delta I_s$* of an Al-Pb diode due to 9.16-GHz longitudinal phonons: trace (a) $T=1.3$°K, trace; (b) $T=2.0$°K. Scales: (a) vertical 2.5 6A/division, (b) vertical 1.25 $\mu$A/division, horizontal 10 $\mu$sec/division. The $dI/dV$ and bias dependence of $\Delta I_s$ for this diode are given in the upper half of Fig. 7.

common source of nonexponential echo decay is due to a variation of the phase of the sound wave across the end face of the rod resulting from nonparallelism of the faces.

The current pulses $\Delta I_s$* also decayed nonexponentially, but the modulation of the decay envelope was not as severe, and the attenuation was less rapid than for the sound echoes detected with the microwave receiver. The modulation pattern in $\Delta I_s$ as well as that of the sound echoes changed when the quartz rod was strained.

We have examined the temperature dependence of the modulation effect from 1.3 to 2.1°K. It was found, in some Al-Pb diodes, that both the decay and modulation pattern of $\Delta I_s$ were strongly temperature dependent, whereas the sound-echoes pattern always remained unchanged with temperature. An illustration of this is seen in Fig. 9 which contains oscillograms of $\Delta I_s$ taken at 1.3 and 2.0°K on the Al-Pb diode whose $I$-$V$ characteristic is given in the upper part of Fig. 7. For example, when the temperature is increased from 1.3 to 2.0°K, the first current pulse decreases by a factor of 2, while the fourth pulse decreases by a factor of 10. On the other hand, the predicted decrease of $\Delta I_s$ calculated from Eqs. (14) and (15) and the measured $I$-$V$ curves is only about 50%. The nonexponential decay of the current pulses may indicate that the tunnel-diode detection is sensitive to variation in the phase of the sound wave across its surface. At the present time, we have been unable to find a satisfactory explanation for this behavior.

## V. CONCLUSION

Although both the bias and power dependence of the extra current $\Delta I_s$ due to longitudinal microwave phonons is described in a qualitative manner by the theories of Tien and Gordon, Cohen, Falicov, and Phillips, and Riedel (extended to sound by Lax and Vernon), there are several serious discrepancies between theory and experiment. In particular, the bias dependence, which was heretofore thought to be adequately described by $\Delta I_s(V)\sim d^2I/dV^2$, has been found, upon closer examination, to exhibit marked departures from this simple law. This effect is most striking in Pb-Pb diodes and is somewhat less apparent when one of the superconductors making up the diode is aluminum. Furthermore, the magnitude of the measured $\Delta I_s$ is much larger than one would predict on the basis of the known acoustic power levels. The tunnel diodes also display a modulation of the current pulse echoes. The shape and the amplitude of this modulation envelope are strongly temperature-dependent. None of this behavior is predicted by the theory.

## ACKNOWLEDGMENTS

We thank G. Weisbarth for his invaluable technical assistance and B. N. Taylor for suggesting to us the method of preparing Pb-Pb diodes. We express our appreciation to R. H. Parmenter and A. Rothwarf for helpful discussions.

## APPENDIX

To evaluate Eq. (14) in the limit $\omega\to 0$ ($\alpha_s\to\infty$), we first expand the function $I(V+n\hbar\omega)$ in a power series in $(n\hbar\omega)$. Equation (14) then becomes

$$I_s(V)=\sum_{r=0}^{\infty}\frac{1}{(2r)!}(\hbar\omega)^{2r}\frac{d^{2r}}{dV^{2r}}I(V)\sum_{n=0}^{\infty}X_n n^{2r}J_n^2(\alpha_s), \quad \text{(A1)}$$

where

$$X_0=1,$$
$$X_n=2, \quad n>0. \quad \text{(A2)}$$

The sum over $n$ can be evaluated using the bilinear expansion[16] of the powers of $\alpha_s$ in terms of $J_n(\alpha_s)$:

$$\alpha_s^{2r+q}=2^{2r+q}r!(r+q)!\sum_{l=0}^{\infty}\frac{(2l+2r+q)(l+2r+q-1)!}{l!(2r+q)!}\times J_{l+r}(\alpha_s)J_{l+r+q}(\alpha_s),$$
$$(q, r=0, 1, 2\cdots{}^{q}\ 2r+q>0). \quad \text{(A3)}$$

Setting $q=0$, we have for $r>0$

$$\frac{(2r)!}{(r!)^2 2^{2r+1}}\alpha_s^{2r}=\sum_{l=0}^{\infty}A_{rl}J_{r+l}^2(\alpha_s), \quad \text{(A4)}$$

where

$$A_{rl}=\frac{(r+l)(l+2r-1)!}{l!}. \quad \text{(A5)}$$

[16] See for example, W. Magnus and F. Oberhettinger, *Formulas and Theorems for the Functions of Mathematical Physics* (Chelsea Publishing Company, New York, 1954), p. 19.

It is convenient to express the coefficient $A_{rl}$ in the form

$$A_{rl}=[l+r]^2[(l+r)^2-1][(l+r)^2-4]\cdots \times[(l+r)^2-(r-1)^2]. \quad \text{(A6)}$$

Then, setting $(l+r)=n$ in the right side of Eq. (A4) we have

$$\frac{(2r)!}{(r!)^2 2^{2r+1}}\alpha_s^{2r}=\sum_{n=r}^{\infty} n^2(n^2-1)(n^2-4)\cdots \times(n^2-(r-1)^2)J_n^2(\alpha_s). \quad \text{(A7)}$$

The lower limit on the summation in Eq. (A7) can be replaced by $n=0$. We then have (for $r>0$)

$$\sum_{n=0}^{\infty} X_n n^{2r} J_n^2(\alpha_s)=\frac{(2r)!}{(r!)^2 2^{2r}}\alpha_s^{2r}+\text{terms proportional to } \alpha_s^{2r-2},\ \alpha_s^{2r-4},\ \text{etc.} \quad \text{(A8)}$$

Substituting Eq. (A8) into Eq. (A1), using the fact that

$$\sum_{n=0}^{\infty} X_n J_n^2(\alpha_s)=1$$

and taking the limit $\alpha_s=(\delta(cs)/\hbar\omega)\to\infty$, one easily obtains the following result for $I_s(V)$:

$$I_s(V)=\sum_{r=0}^{\infty}\frac{1}{(r!)^2}\left(\frac{[\delta(cs)]}{2}\right)^{2r}\frac{d^{2r}I(V)}{dV^{2r}} \quad \text{(A9)}$$

or

$$I_s(V)=I_0(\delta[cs]d/dV)I(V), \quad \text{(A10)}$$

where $I_0$ is the modified Bessel function of order zero.

*Note added in proof.* It has now been established that the high $T_c$ of the aluminum films used in the present work results from contamination by oxygen. The effect of oxygen on the $T_c$ of metal films is described by B. Abeles, R. W. Cohen, and G. W. Cullen in Phys. Rev. Letters **17**, 632 (1966).

PHYSICAL REVIEW VOLUME 151, NUMBER 1 4 NOVEMBER 1966

# Decay Features of Positrons in Semiconductors*

G. FABRI, G. POLETTI, AND G. RANDONE
*Centro Informazioni Studi Esperienze, Milano, Italy*
(Received 20 June 1966)

Positron lifetime measurements in some typical semiconductors are reported. In every case the decay displays two components, the longer one being of the order of $\tau_2=10^{-9}$ sec and having an intensity of a few percent. Measurements on neutron-damaged samples show that both components are sensitive to the presence of lattice defects. Moreover, at least in the case of silicon, the long-lifetime component is lacking when a high electric field is applied to the sample. Also, the presence of a high oxygen concentration in gallium arsenide and in silicon is effective in preventing annihilations through the $\tau_2$ lifetime.

## INTRODUCTION

POSITRON lifetime measurements in germanium[1] established that the decay is simple, displaying only one lifetime; moreover, the shape of angular correlation spectra in germanium and silicon,[2-4] substantially an inverted parabola, led to the conclusion that positrons annihilate with nearly free electrons, without formation of positronium-like bound states. On the basis of these results, one could suppose that positron annihilation in semiconductors is likely to display features similar to those in metals. However, in semiconductors it is possible to make the conduction-electron concentration vary over a wide range, both by doping the samples and, in nonequilibrium conditions, by applying an electric field to them.

It seems therefore worthwhile to examine positron decay features in a few typical semiconductors; silicon, germanium, boron, gallium arsenide, and silicon carbide have been tested.

## EXPERIMENT AND RESULTS

The Vernier time sorter has already been described in previous work.[5] The over-all resolution defined by the full width at half-maximum of a prompt-coincidence curve was $8.5\times10^{-10}$ sec.

The source, about 20 $\mu$Ci of carrier-free $Na^{22}$, was deposited directly onto the samples, which were in the shape of disks cut from single crystals, except for boron and silicon carbide, which were polycrystalline.

* A few preliminary results from this study have been presented at the Positron Annihilation Conference, Detroit, 1965.

[1] G. Jones and B. Warren, Can. J. Phys. **39**, 1520 (1961).
[2] G. Lang and S. De Benedetti, Phys. Rev. **108**, 914 (1957).
[3] A. T. Stewart, Can. J. Phys. **35**, 168 (1957).
[4] P. Colombino, B. Fiscella, and L. Trossi, Nuovo Cimento **31**, 950 (1964).
[5] E. Germagnoli, G. Poletti, and G. Randone, Phys. Rev. **141**, 419 (1965).

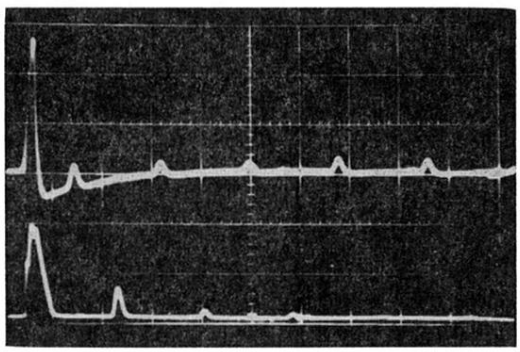

FIG. 2. Typical oscillogram of tunnel-diode current pulses $\Delta I_s^*$ at output of pulse amplifier (upper trace) and of sound echoes detected by microwave receiver (lower trace). Horizontal scale 5 $\mu$sec/division, diode Al-Pb, thickness of Pb strip 7000 Å, $T=1.3°$K.

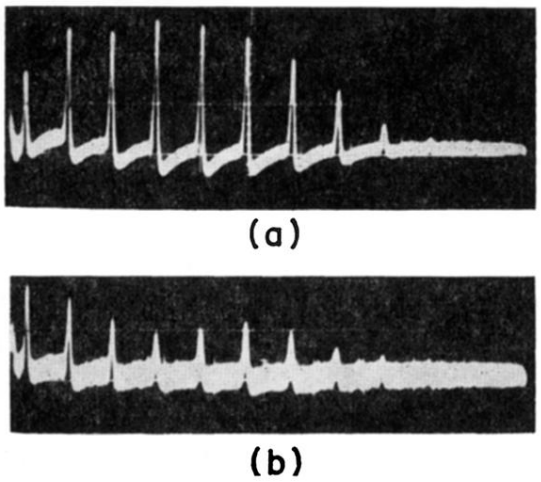


FIG. 9. Oscillograms of current pulses $\Delta I_s^*$ of an Al-Pb diode due to 9.16-GHz longitudinal phonons: trace (a) $T=1.3°K$, trace; (b) $T=2.0°K$. Scales: (a) vertical 2.5 6A/division, (b) vertical 1.25 $\mu$A/division, horizontal 10 $\mu$sec/division. The $dI/dV$ and bias dependence of $\Delta I_s$ for this diode are given in the upper half of Fig. 7.